Journal of Hazardous Materials, 16 (1987) 9–20
Elsevier Science Publishers B.V., Amsterdam — Printed in The Netherlands

THE THORNEY ISLAND CONTINUOUS RELEASE TRIALS: MASS AND FLUX BALANCES

A. MERCER and C. NUSSEY

Health and Safety Executive, Safety Engineering Laboratory, Broad Lane, Sheffield S3 7HQ (Great Britain)

(Received November 11, 1986; accepted April 29, 1987)

Summary

This paper shows that by making a number of assumptions and judgements reasonably good mass and flux balances are obtained for the Thorney Island continuous release trials, thus confirming the overall consistency of the data.

1. Introduction

The objectives, and experimental design, of the three continuous release trials (Trials 45–47) conducted at Thorney Island, together with a summary of the results are presented elsewhere in this volume [1]. In this paper we describe the work conducted to determine mass-flux and mass balances for the trials.

The purpose of conducting mass and flux balances was to provide an overall measure of the consistency of the experimental data.

In order to conduct a mass-flux balance in which the total flux of gas across a plume section is compared with the initial release rate of gas (ca. 10.4 kg/s), information on the velocity and concentration distributions within the plume is required. Examination of the data books [2] shows that 3 and 5 sonic anemometers were within the plumes for Trials 45 and 47, respectively. Information on the velocity distribution is therefore very limited and the methods adopted for conducting mass-flux balances are constrained by this fact. These data are therefore augmented by considering plume arrival and departure times.

The data base of concentration records is more extensive; typical concentration records are given by McQuaid [1]. The form of the concentration record depends on the sensor location; in particular there can be significant variation with height. (Throughout this report gas concentrations are expressed as a percentage of the initial concentration.)

Data for Trial 46 is too limited, so it is not considered further. The methods adopted are described in Section 2, and the results are discussed in Section 3.

Details of a mass balance for Trials 45 and 47 are presented in Section 4 and Section 5 draws some conclusions.

2. Volumetric flux balance—Method

Examination of the concentration records showed that in general the variation in concentration levels across the plume are not appreciable in the near field, but that the variations become more appreciable further downwind. However, because of the distribution of sensors, the spatial variation of concentration within the plume is not well defined. These general observations led us to adopt two approaches to obtain a mass-flux balance; one based on the assumption of a uniform concentration distribution across the plume and one based on a Gaussian distribution of concentration across the plume. In both cases the flux balances are obtained at a number of plume sections that are normal (or nearly so) to the mean wind direction, the sections being chosen to include as many gas sensors as possible.

Assuming a steady state, the mass transport rate, $\dot{m}$, of contaminant gas (of initial density, ρ_0) across a section S normal to the plume is,

$$\dot{m} = \int_s \rho_0 C\, U \, \mathrm{d}A \tag{1a}$$

$$= \rho_0 \int_s C\, U \, \mathrm{d}A \tag{1b}$$

$$= \rho_0 \dot{q} \tag{1c}$$

For a 'perfect' experiment, the mass transport rate so defined must equal the mass transport rate of the contaminant gas at the source, $\dot{M}$. Clearly, $\dot{M} = \rho_0 \dot{Q}$, where $\dot{Q}$ is the volumetric flow rate of contaminant gas at the source. A test of the consistency of the experiment then is to compare $\dot{q}$ with $\dot{Q}$. We call this, a volumetric 'flux' balance.

The volumetric flux $\dot{q}$ across a plume section is

$$\dot{q} = \int_{z=0}^{h} \int_{y=-l}^{l} C(y,z)\; U(y,z)\; \mathrm{d}y\, \mathrm{d}z \tag{1d}$$

Under the assumption that the concentration and velocity distributions laterally are uniform across each plume section, eqn. (1d) can be written,

$$\dot{q}(x) = 2l \int_{z=0}^{h} C(z)\; U(z)\; \mathrm{d}z \tag{2}$$

Thus in order to evaluate the volumetric flux through a section we need to estimate $C(z)$ and $U(z)$ for that section. A Gaussian distribution has been fitted to the concentration profile in the vertical direction; this is described in Section 2.1. Since the sections are chosen to maximise the information on the

concentration distribution, reasonable estimates of $C(z)$ can be made. This is not the case for $U(z)$ in view of the limited number of sonic anemometer records available. In consequence we assumed that $U(z)$ can be replaced by a velocity $\bar{U}$, averaged over the depth of the plume. This is discussed in Section 2.2.

Assuming that the contribution from the tail of the Gaussian distribution is small, eqn. (2) becomes,

$$\dot{q}(x) = 2l\,\bar{U}\,C_m \int_0^\infty \exp\left(-\frac{z^2}{2\,\sigma_z^2}\right) dz \tag{3a}$$

$$= 2l\,\bar{U}\,C_m \sqrt{\frac{\pi}{2}}\,\sigma_z \tag{3b}$$

Under the alternative assumption that the concentration distributions vertically and horizontally across the plume are Gaussian and that the contributions from the tails of the Gaussian distributions are small we can write,

$$\dot{q}(x) = \bar{U}\,C_m \int_{-\infty}^{\infty} \exp\left(-\frac{y^2}{2\,\sigma_y^2}\right) dy \cdot \int_0^\infty \exp\left(-\frac{z^2}{2\,\sigma_z^2}\right) dz \tag{4a}$$

$$= \bar{U}\,C_m\,\pi\,\sigma_y\,\sigma_z \tag{4b}$$

A value of σ_y at each section was obtained by equating the concentration at the assumed plume width (see Section 2.3) to 0.1%, the lower limit of resolution of the sensors and by taking the value of C_m from the vertical profiles.

2.1 Vertical concentration profiles

The concentration profiles were determined as follows. For each gas sensor on each mast in a particular section the average concentration over a period for which the concentration was judged to be 'steady' was determined by eye from the hard-copy data books. For sensors in the near field such a 'steady' concentration was quite well defined. It became less so as the distance from the source increased; see McQuaid and Roebuck [3]. For some records, the concentration appears to be on more than one level so a range of 'mean' concentrations were estimated. In consequence, more than one profile of the Gaussian form can be fitted to the data at these locations. It will be seen, however, that, on the whole, the mass-flux balances are not greatly affected by these difficulties.

Sections were chosen normal (or nearly so) to the mean wind direction so as to include as many sensors as possible. In some cases the data was augmented by linear interpolation between sensors in a direction as close to the mean wind direction as possible. The locations of the sections are given in Table 1 and are shown in Figures 1 and 2 for Trials 45 and 47, respectively.

TABLE 1

Location, dimensions and Richardson's number for the sections at which mass flux balances were conducted

	Section	Downwind distance, m	Plume height,[a] m	Plume width, m	Ri[b]
Trial 45	1	36	0.97	109	82
	2	43	1.9 -2.60	118	134
	3	62	1.00-1.58	140	74
	4	107	1.41-2.58	182	39
	5	203	2.82-6.63	247	29
	6	250	4.91-6.95	274	20
	7	467	5.45-7.55	371	5
Trial 47	1	38	1.10	187	340
	2	44	1.04-1.95	190	383
	3	61	1.09-1.66	200	296
	4	126	1.78-4.14	226	44
	5	202	2.81	249	65

[a]The range of plume heights ($=2.15\ \sigma_z$) correspond to the range of vertical profiles at each section.
[b]The Richardson number has been calculated using the mean of the plume heights.

2.2 Plume advection speed

The plume advection speed was determined from a consideration of the velocity profile at the meteorological station (the 'A'-mast), data from the anemometers within the plume and the plume front and trailing edge speeds. Each of these approaches in itself is not sufficient to give a reliable value for the advection speed. It is by viewing the results in toto that a representative value is obtained.

The hard-copy data books were used to obtain average values (estimated by eye) of wind-speed from the sonic anemometers on the 'A'-mast and on the three masts indicated on Figs. 1 and 2. In the case of the A-mast, data from four cup-anemometers were also available. A logarithmic velocity profile, for neutral stability conditions, $U=(u_*/k)\ \ln\ (z/z_0)$ was fitted to the data using values averaged over a 10 min period covering that in which gas was being released. The atmospheric stability for Trials 45 and 47, was judged to be Pasquill category E/F [1]. In view of the difficulties in determining z_0 and the Monin–Obukhov length, L (see Puttock [4]), it was considered that fitting a velocity profile for neutral conditions was adequate for both trials. The results for Trials 45 and 47 are shown in Figs. 3 and 4, respectively, together with the wind speeds (10 min average) from the anemometers on the masts at (400,275), (450,275) and (500,275). These figures indicate that at a height of 1 m (about

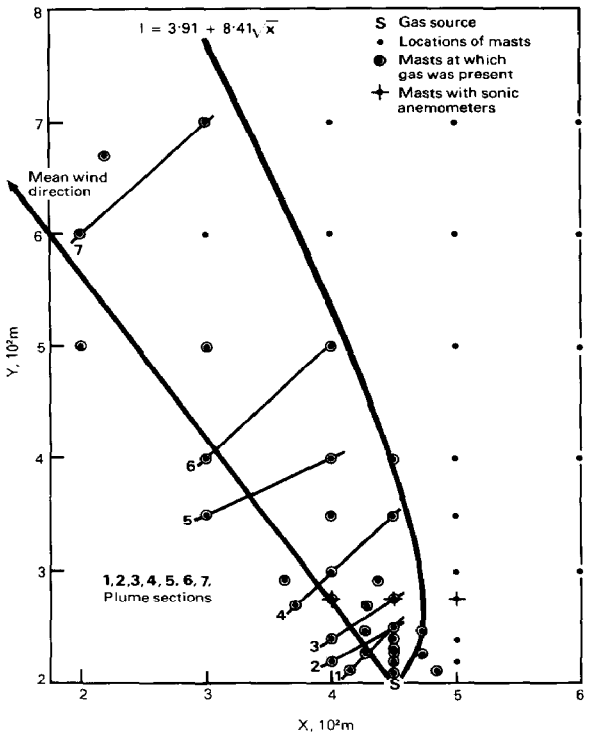

Fig. 1. Mast array, plume sections and plume outline; Trial 45.

half the depth of the plumes) the velocities were about 0.9–1.4 m/s for Trial 45 and 0.5–1 m/s for Trial 47.

Further information on the plume speed can be obtained by considering the plume front and trailing edge speeds. For gas sensors within the sector defined by the mean wind direction $\pm 10°$, the arrival and departure times of gas were determined at each height. The arrival time t_a (s) is taken to be the time at which the concentration rises above 0.1%, the lower limit of resolution of the sensors. This definition can lead to a difference of about 60 s in comparison to the arrival times based on an estimate of the time at which the concentration level begins to depart from the base line. The time t_d (s) is the latest time at which the concentration falls below 0.1%. The arrival time is quite well defined, the departure time not so. The plume front and trailing edge speeds were determined from the slope of a straight line fit to the plot of downwind distance v. arrival and departure times, respectively. These plots show a degree of scatter and, at short distances, a consistent deviation which is attributed to plume inertia. In general, the plots of downwind distance v. departure time showed more scatter.

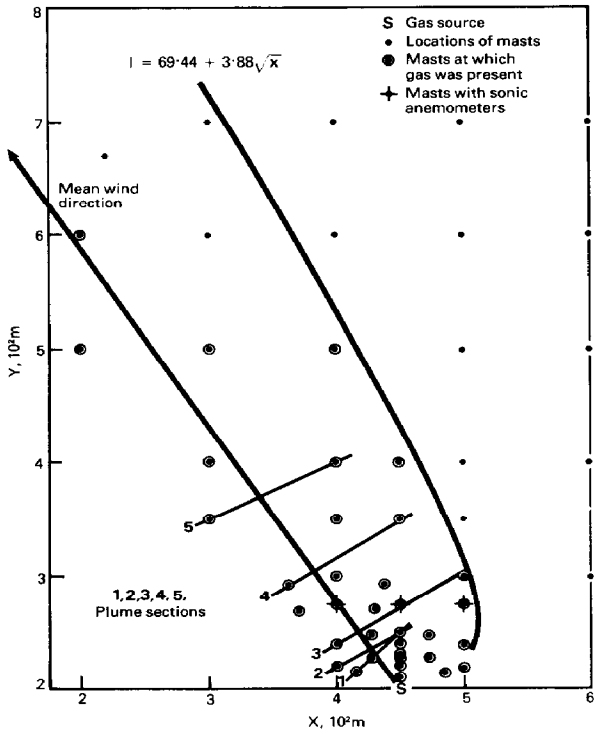

Fig. 2. Mast array, plume sections and plume outlines; Trial 47.

This exercise was repeated for all sensor heights and trials. The results are summarised in Figs. 3 and 4 for convenience.

Taking all the results together the advection speeds for Trials 45 and 47 are about 0.9 and 0.6 m/s, respectively. These 'average' values are adopted for use with eqns. (3b) and (4b).

2.3 Determination of the plume width

It transpires that the plume width cannot be determined directly from the trials data. The reason for this is that in Trials 45 and 47, when the plume travelled to the left of the range centre-line there were no gas sensors on the left of the plume that did not see gas so that the left-hand side of the plume is indeterminate. However, if the plume is assumed to be symmetrical about the mean wind direction, the pattern of sensors which saw gas can be used to estimate the plume half-width.

Inspection of this pattern, together with a judgement as to which sensors were near to the plume boundary, suggested that the plume half-width, l, behaved as $\sqrt{x}$, where x is the downwind distance along the mean wind direction. For each of the Trials 45 and 47, a graph of l against $\sqrt{x}$ was plotted and

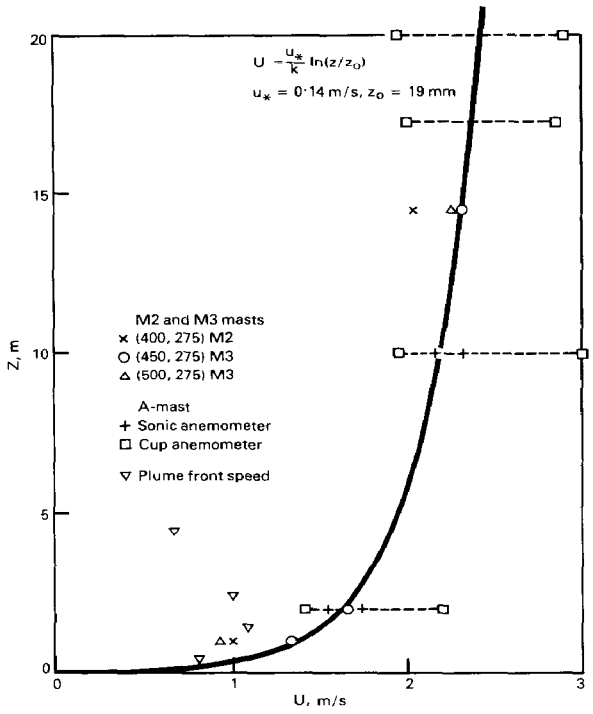

Fig. 3. Plume velocities and velocity profile at the A-mast; Trial 45.

the best straight line fitted. The resulting plume boundaries are shown in Figs. 1 and 2 and the values of the plume widths ($2l$) are given in Table 1. The table also shows the location of each plume section, its height (estimated from the Gaussian profiles as the height equal to 2.15 σ_z) and the local Richardson number, $Ri = g\Delta\rho h/(\rho_a u_*^2)$. (The determination of u_* is described in Mercer and Davies [5].)

3. Results

The values of the volumetric flux ratio, $\dot{q}/\dot{Q}$, under the assumption that the concentration distribution is uniform across the width of the plume, are given in Table 2 (column a). It can be seen that in general the predicted fluxes are overestimates but particularly so in the near field. The discrepancy in the near field cannot be attributed to erroneous values of l, because the values used are likely to be under-estimates due to lateral spreading. The values of $\bar{U}$ could be too high, but there is no evidence to suggest that the actual values in the near field are greater than those used by the required factor of 2 or 3. It thus appears that the main discrepancy is due to the assumption of a uniform concentration distribution across the width of the plume. Alternatively, therefore, we present

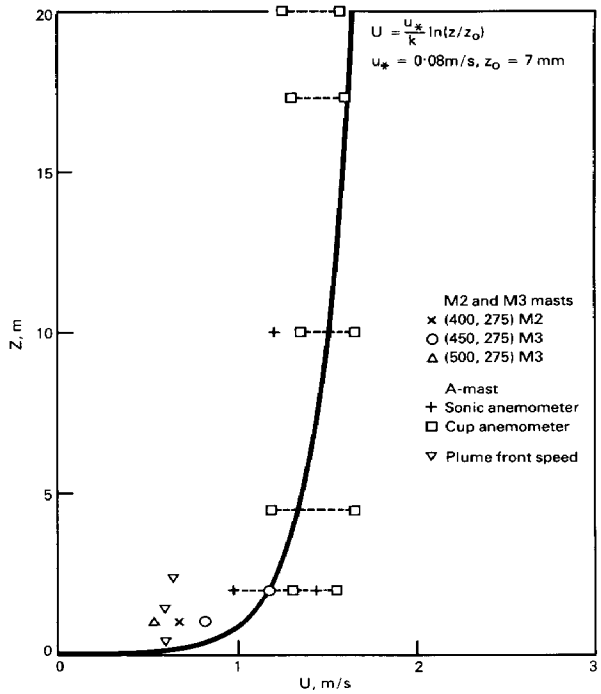

Fig. 4. Plume velocities and velocity profile at the A-mast; Trial 47.

results based on the assumption of a Gaussian distribution of concentration across the plume (as explained in Section 2); these are given in Table 2 (column b).

Table 2 (column b) shows that in general the flux balance is improved. For most sections the flux balance is within $\pm 50\%$. Taking the results of Table 2 together it is our judgement that there is evidence to suggest that the flux balance is satisfied to the expected accuracy for this type of experiment.

4. Mass balances for Trials 45 and 47

Since gas was released at a steady rate of about 10.36 kg s^{-1} the mass of gas within the plume at any time is known within the experimental error ($\pm 2\%$, [3]). A mass balance can therefore be conducted by estimating the plume outline, the concentration distribution within the volume of the plume, and performing the necessary integration.

The plume outline at a particular time was estimated from the arrival times of gas at particular masts. The concentration distribution was obtained by dividing the plume into a number of volume elements formed by taking horizontal and vertical sections through the plume that resulted, as far as possible,

TABLE 2

Values of the volumetric flux ratio, $\dot{q}/\dot{Q}$, for (a) uniform and (b) Gaussian cross-wind distribution

Plume section	Downwind distance, m	a	b
Trial 45	$\bar{U} = 0.9$ *m/s*	$\dot{Q} = 260$ *m³/min*	
1	36	2.19	0.86
2	43	2.77-3.90	1.08-1.60
3	62	1.46-2.55	0.61-1.06
4	107	1.50-2.08	0.68-0.97
5	203	1.07-1.76	0.66-0.93
6	250	0.81-1.89	0.57-1.15
7	467	0.61-1.10	0.69-0.87
Trial 47	$\bar{U} = 0.6$ *m/s*	$\dot{Q} = 250$ *m³/min*	
1	38	3.53	1.35
2	44	3.32-4.85	1.28-1.91
3	61	2.86-3.55	1.13-1.43
4	126	0.26-0.77	0.21-0.41
5	202	0.90	0.48

Note: The range of values in columns a and b correspond to the range of vertical profiles at each section.

in a gas sensor being near to the centre of the volume element. The horizontal sections were taken at heights of 0.8, 3.4, 5.4 and if necessary 7.4 m so that mean concentrations in the corresponding elemental volumes could be obtained from the appropriate gas sensor records at heights of 0.4, 1.4, 2.4, 4.4, and 6.4 m, respectively. Locations of the vertical sections were based on the ground-level plume outline in relation to the mast array. The fact that gas spread upwind of the source was taken into account.

The method was applied to Trials 45 and 47 at a time of 400 s from the start of the release. Thus the mass of gas in the plume at the time was 4144 ± 83 kg, say 4150 kg. Examination of the data books indicated that an appreciable proportion of this mass would be in the near field and in the lowest two horizontal slices. An attempt was therefore made to use relatively small elemental volumes in the near field. In the far field there are fewer masts and the volume elements were of necessity larger. The results are not sensitive to the maximum height being restricted to 7.4 m as the mass of gas in the uppermost elemental volumes was considerably less than the accuracy expected of the method. For Trial 47 no gas was at this level and for Trial 45 only about 0.6% of the released material was estimated to lie between 5.4 and 7.4 m at a time of 400 s.

For Trial 45, 22 elements were used at the lowest level, and 55 in total. The

estimated mass in the plume is 3431 kg, which compares favourably (i.e. within 17.3%) with the expected quantity of 4150 kg. The results for Trial 47 at 400 s were even better, the estimates being 3769, i.e. within 9.2%.

One interesting observation from this approach is that the estimates of the plume outlines at 400 s for Trials 45 and 47 are relatively small compared to that which would be drawn by consideration only of the masts that were immersed in gas, i.e. without regard to the arrival times. This was particularly so for Trial 47, so the exercise was repeated for a time of 560 s; a significantly larger plume outline was obtained. These observations indicate that the steady state plume widths may take some time to establish.

5. Conclusions

1. One of the main uncertainties in conducting the flux balance stemmed from the estimation of the plume advection speed. Examination of the data from sonic anemometer records within the plume tended to suggest that estimates based on the front and trailing edge speeds could be adopted. Although the plots of arrival and departure times showed much scatter the indications were that the corresponding speeds were fairly similar and typically 0.9 and 0.6 m/s for Trials 45 and 47.

2. Adoption of these values for the plume advection speed and either a uniform vertical concentration distribution across the plume or a Gaussian concentration within a plume section lead to volumetric flux balances that were, except in the near field, within a factor of two of the expected value.

3. For Trials 45 and 47 an independent mass balance was conducted by estimating the plume outline at a particular time and dividing this up into elemental volumes centred, as far as possible on sensors that had detected gas. This method gave results that underestimated the mass of gas in the plume by about 20%.

4. Examination of the gas sensor records indicate that gas was present at heights greater than indicated by visual observation of the plume. There was a particularly steep concentration gradient in the near field – the concentration levels at 0.4 m height being about an order of magnitude greater than those observed at 1.4 and 2.4 m. In the far field the concentrations at heights of 0.4 and 2.4 m are fairly similar or within a factor of about 2.

5. Information on plume width and its variation with distance as obtained from the concentration data base is imprecise because of the spatial separation of masts, but mainly because parts of the plumes were outside the mast array. Estimates of the plume half width could be obtained by assuming that the plume was symmetrical about the mean wind direction. The estimated plume outline at different times indicates that it could take some time to establish a steady state beyond about 100 m downwind, particularly in low wind speeds.

6. Examination of the concentration records showed that there was significant lateral and upwind spreading at the source.

Acknowledgements

The authors acknowledge the assistance of M. Knowles in the preparation of this paper.

Notation

$C(x,y,z)$	gas concentration, expressed as a percentage of that of the released gas mixture
C_m	gas concentration at ground level on the plume centre-line, i.e. $C(x,0,0)$
dA	element of area of cross-section
h	depth of plume
k	von Karman's constant, equal to 0.4
l	cross-wind plume half-width
L	Monin–Obukhov length
$\dot{M}$	mass-flow rate of gas at the source
$\dot{m}$	mass-flow rate of gas across a section of the plume
$\dot{q}$	volumetric flow rate of gas across a section of the plume
$\dot{Q}$	volumetric flow rate of gas at the source
Ri	local value of the Richardson number, $g(\Delta\rho/\rho_a)/(h/u_*^2)$
t_a, t_d	plume arrival and departure times
u_*	friction velocity
$U(x,y,z)$	downwind velocity
$\bar{U}$	mean plume advection speed
x, y, z	Cartesian co-ordinate system, using site axes to specify sensor locations, but using an axis aligned with the mean wind direction for the description of the plume geometry
z_0	roughness length
ρ	density of gas at a section of the plume
ρ_0	density of initial gas mixture
ρ_a	density of air
σ_y	horizontal dispersion coefficient
σ_z	vertical dispersion coefficient

References

1 J. McQuaid, Design of the Thorney Island continuous release trials, J. Hazardous Materials, 16 (1987) 1–8.

2 Health and Safety Executive, Data for heavy gas dispersion trials, Thorney Island, 1982–83, Research and Laboratory Services Division, Health and Safety Executive, Sheffield S3 7HQ 1985.
3 J. McQuaid and B. Roebuck, Large scale field trials on dense vapour dispersion, Report No. EUR 10029, Commission of the European Communities, Brussels, 1985.
4 J.S. Puttock, Analysis of meteorological data for the Thorney Island Phase I trials, J. Hazardous Materials, 16 (1987) 43–74.
5 A. Mercer and J.K.W. Davies, An analysis of the turbulence records from the Thorney Island continuous release trials, J. Hazardous Materials, 16 (1987) 21–42.